Glycosylation Characterization of Human and Porcine Fibrinogen Proteins by Lectin–Binding Biophotonic Microarray Imaging

ARTICLE *in* ANALYTICAL CHEMISTRY · DECEMBER 2013

Impact Factor: 5.64 · DOI: 10.1021/ac402872t · Source: PubMed

4 AUTHORS, INCLUDING:

Martin Weissenborn
The University of Manchester
13 PUBLICATIONS **114** CITATIONS
SEE PROFILE

Sabine Flitsch
The University of Manchester
204 PUBLICATIONS **3,857** CITATIONS
SEE PROFILE

Andrew Mark Shaw
University of Exeter
62 PUBLICATIONS **697** CITATIONS
SEE PROFILE

analytical chemistry

Article

pubs.acs.org/ac

Glycosylation Characterization of Human and Porcine Fibrinogen Proteins by Lectin-Binding Biophotonic Microarray Imaging

Rouslan V. Olkhov,[†] Martin J. Weissenborn,[‡] Sabine L. Flitsch,[‡] and Andrew M. Shaw*,[†]

[†]College of Life and Environmental Sciences, University of Exeter, Exeter, Devon EX4 4QD, United Kingdom

[‡]School of Chemistry & MIB, The University of Manchester, Manchester, North West England M1 7DN, United Kingdom

ABSTRACT: Lectin binding has been studied using the particle plasmon light-scattering properties of gold nanoparticles printed into an array format. Performance of the kinetic assay is evaluated from a detailed analysis of the binding of concanavalin A (ConA) and wheat germ agglutinin (WGA) to their target monosaccharides indicating affinity constants in the order of K_D ~10 nM for the lectin-monosaccharide interaction. The detection limits for the lectins following a 200 s injection time were determined as 10 ng/mL or 0.23 nM and 100 ng/mL or 0.93 nM, respectively. Subsequently, a nine-lectin screen was performed on the porcine and human fibrinogen glycoproteins. The observed spectra of lectin-protein specific binding rates result in characteristic patterns that evidently correlate with the structure of the glycans and allow one to distinguish between glycosylation of the porcine and human fibrinogens. The array technology has the potential to perform a multilectin screen of large numbers of proteins providing information on protein glycosylation and their microheterogeneity.

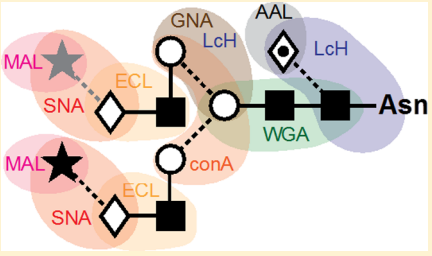

The analysis of protein glycosylation has become an important facet of biopharmaceutical production as glycoproteins make up more than one-third of approved biopharmaceuticals.[1−3] The development of the tools for structure determination of glycans is also identified as a high priority target by the National Academy of Sciences.[4] For glycoprotein hormones, such as human erythropoietin, glycosylation determines pharmacokinetic and pharmacodynamic profiles.[5,6] The plethora of therapeutic antibodies currently in the clinic and development need to be expressed with precise glycosylation patterns for correct therapeutic function.[7] Given the dynamic character of glycosylation during and after protein translation in the cell, tight quality control of biopharmaceutical production is needed with fast, efficient, and precise analytical techniques to monitor protein glycosylation.

Glycosylation is the most abundant post-translational modification (PTM) in nature, where glycans are attached to proteins or lipids.[8] The glycosylation is highly diverse and is therefore used as a unique pattern for cell-cell recognition.[9] Protein glycosylation is important for the refolding, solubility, and stability of the proteins,[10] and defects in glycosylation are observed in diseases such as allergies or muscular dystrophies.[11,12] The determination and detection of different glycosylation is nontrivial and laborious and requires a complex set of analytical techniques.[13] Among them are nuclear magnetic resonance,[14] mass spectrometry[15] in combination with gas and liquid chromatography,[16] and eastern or lectin blotting.[17,18] An important tool for characterizing glycans is the specific binding of lectins, which are commercially available and can be highly selective for mostly terminal saccharides.[19−22] Fluorescence-assisted lectin microarrays emerged recently and offer two advantages over chromatography and mass spectrometry techniques: speed of high throughput screening and an ability to profile glycosylation without liberation glycans from the complex biological samples, including cells and tissues.[23,24] In combination with surface plasmon resonance (SPR),[25] lectins can provide useful quantitative data on protein glycosylation without the need for the more conventional fluorescent labeling of probes.[22,26] Using the SPR label-free technology in an array format allows the study of large numbers of carbohydrate-protein interactions including determination of binding kinetics, affinity and avidity constants, and relative energies of interactions.

We have developed an SPR related label-free biophotonic sensor array technique[27] for the analysis of proteins from solution, including antibodies from complex fluids.[28] The technique uses the sensitivity of the light scattering properties of the gold nanoparticle localized surface plasmons to provide intensity changes observed in real time with a video camera. The gold nanoparticle array spots can be functionalized by self-assembling monolayers (SAMs) which carry a terminal carboxylic group (linker) for chemical modification and a terminal hydroxyl group (spacer), respectively.[29,30] The carboxylic group can be used to couple various different chemically modified sugars onto the surface.[31] The hydroxyl group carrying the molecule spacer allows spacer dilutions, which is important to understand the different affinities of lectins, both to high and low concentrated sugars on the surface.[32,33] Also larger molecules, such as glycoproteins, can be coupled into the SAMs, and their glycosylation can be studied.

Received: September 9, 2013
Accepted: November 29, 2013
Published: November 29, 2013

   dx.doi.org/10.1021/ac402872t | *Anal. Chem.* 2014, 86, 621−628

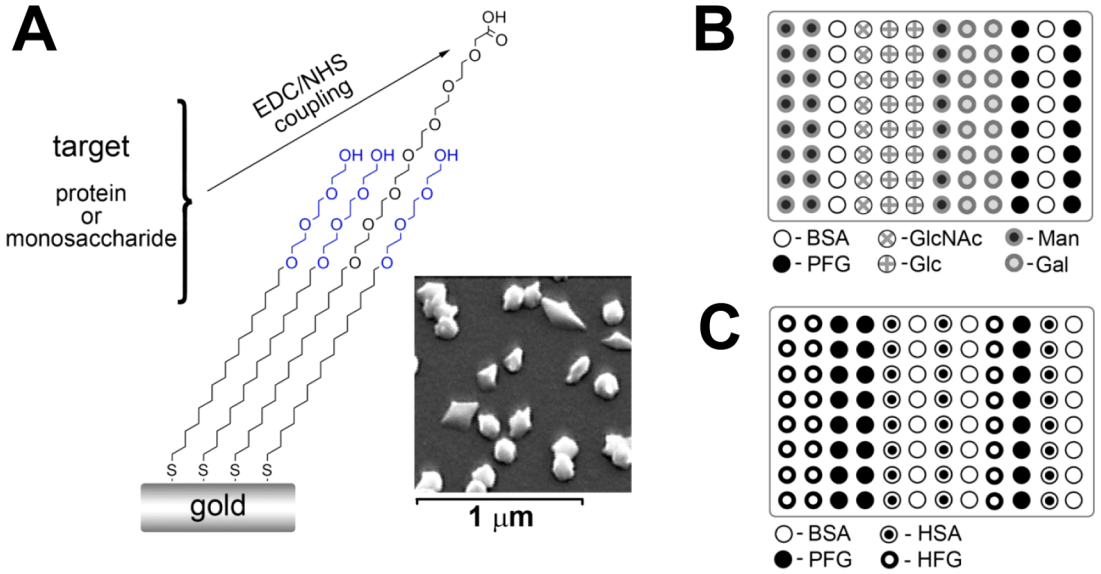

Figure 1. Sensor preparation details: (A) biofunctionalization of sensor arrays by EDC/NHS coupling to carboxylic groups present in self-assembling monolayers (SAMs) (left). The hydroxyl and carboxyl terminal molecules form the SAMs on gold nanoparticles shown in SEM image (right); array print legends used in preliminary lectin-monosaccharide binding assays (B) and in fibrinogen glycosylation screening (C).

Here, we report the first analysis for the label-free biophotonic imaging detection of glycans on the glycoprotein fibrinogen. The β and γ subunits of fibrinogen contain N-glycosylation sites occupied by biantennary glycans, with porcine and human oligosaccharide structures different by a single fucose.[34−36] For proof-of-principle studies, the lectin binding specificities and kinetics were first studied using monosaccharides. The optimized protocols were subsequently applied to characterize the glycosylation of the porcine and human fibrinogens. This new technique enables the fast screen of protein glycosylation and could therefore become valuable in the quality control of glycosylated biopharmaceuticals.

EXPERIMENTAL METHODS

Reagents. Self-assembling monolayer (SAM) components, HS-$(CH_2)_{17}$-$(OC_2H_4)_3$-OH (used as a "spacer") and HS-$(CH_2)_{17}$-$(OC_2H_4)_6$-OCH_2COOH (used as a "linker"), were obtained from ProChimia Surfaces (Poland). *N*-(3-Dimethylaminopropyl)-*N*′-ethylcarbodiimide hydrochloride (EDC), *N*-hydroxysuccinimide (NHS), bovine serum albumin (BSA), human serum albumin (HSA), fibrinogen from pig plasma (PFG), and fibrinogen from human plasma (HFG) were obtained from Sigma-Aldrich. The biotinylated lectins from *Erythrina cristagalli* (ECA), *Lens culinaris* (LcH), *Galanthus nivalis* (GNA), *Arachis hypogaea* (peanut) (PNA), *Sambucus nigra* (SNA), *Maackia amurensis* (MAL), and *Aleuria* aurantia (AAL) were kindly provided by Galab. The fluorescein-labeled concanavalin A (ConA) lectin and wheat germ agglutinin (WGA) were acquired from Vector Laboratories. The experiment does not use the label as part of the detection process: the lectins were readily available from the supplier and at high purity. Aminoethyl glycoside derivatives of the monosaccharides α-D-mannose (αMan), β-D-glucose (βGlc), β-D-galactose (βGal), and *N*-acetyl-β-D-glucosamine (βGlcNAc) were prepared by glycosylation methods reported elsewhere.[31] The standard running and dilution buffer (PBST) was phosphate buffered saline, containing 5×10^{-5} w/w Tween 20 surfactant and 1 mM both $CaCl_2$ and $MgCl_2$ to stabilize the lectins. Aqueous 100 mM phosphoric acid solution, pH 1.9, was used as the regeneration buffer.

Sensor Array Preparation. The manufacture of the gold nanoparticle biophotonic arrays used in these experiments is described in detail elsewhere.[27,37] Briefly, the rectangular 12 × 8 sensor arrays are inkjet printed with a 300 μm pitch between the spots and a spot diameter of 200 μm, Figure 1. Each spot is printed with seed nanoparticles 4 nm in diameter, the arrays are removed from the printer, and placed in a growth solution to grow truncated polyhedral gold nanoparticles with an approximate diameter of 120 nm. These particles are present with a surface density of approximately 25% and are the plasmon light-scattering centers for assays. The arrays are then returned to the inkjet printer for biofunctionalization.

Analyte binding specificity is introduced by functionalization of the gold surface with a particular monosaccharide or a protein. Before the functionalization, the sensor surface was activated by coating the gold nanoparticles with a mixed SAM of linker and spacer alkanethiol molecules, Figure 1A, followed by activation of the linker carboxylic groups with the common EDC/NHS chemistry to produce succinimide esters reactive toward primary amino groups. Five mixtures with different ratios of linker to spacer SAM components were used: 1:4, 1:10, 1:100, 1:1000, and 1:2500.

Four monosaccharides, αMan, βGal, βGlc, and βGlcNAc, and four proteins, bovine and human albumins BSA and HBA and porcine and human fibrinogens HFG and PFG, were inkjet printed at 2 mg/mL concentration onto activated sensors according to the legends shown in Figure 1B,C, incubated overnight at room temperature, rinse washed with deionized (DI) water, and stored at 4 °C until used.

Lectin Binding Kinetic Assay. The biophotonic microarray sensor imaging technique is described in detail elsewhere.[37] The sensor arrays are rehydrated in PBST buffer for 15 min, washed with regeneration buffer, blocked with 2 mg/mL solution of BSA in PBST for 10 min, washed again with regeneration buffer, and finally stabilized in PBST running buffer flow. An injection of double concentrated PBS buffer was performed to establish the dependence of the array spots

dx.doi.org/10.1021/ac402872t | *Anal. Chem.* 2014, 86, 621−628

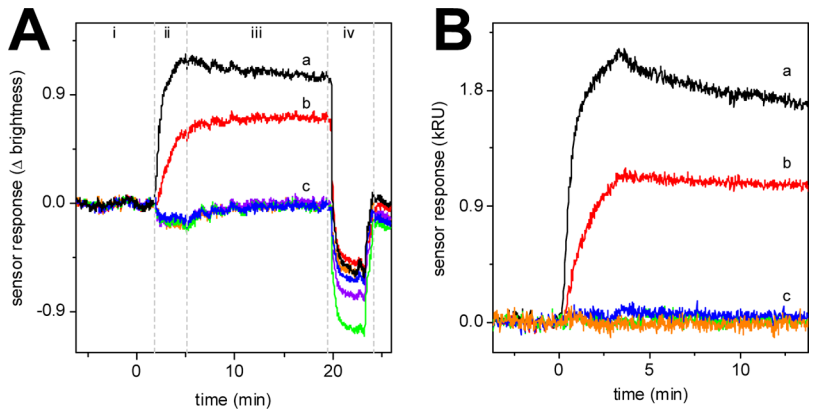

Figure 2. Example of the experimental sensogram data recorded in an assay of 2 μg/mL ConA lectin sample: (A) averaged scattering intensity changes recorded from 8 or 16 arrays spots functionalized with the same material showing the experimental phases (i) baseline, (ii) association, (iii) dissociation, and (iv) regeneration; (B) data from panel A is referenced against the BSA control channel to compensate for the differences in refractive indices of running buffer and lectin samples. The control channel further corrects for temperature variations and light source intensity instabilities. The signal scale is converted into response units, and the injection time lag is removed. The marked traces on both panels are: a, αMan; b, PFG; overlapping c, βGal, βGlc, and βGlcNAc and BSA (panel A only).

Table 1. Parameters of the ConA-αMan Interaction Derived from Assays on Sensor Surfaces with Varying SAM Composition[a]

linker/spacer	$10^{-4} \times k_a$ (M^{-1} s^{-1})	$10^4 \times k_d$ (s^{-1})	K_D (nM)	ϑ_{max} (kRU)	$-\Delta G$ (kJ M^{-1})
1:4	4 ± 3	10 ± 0.3	24 ± 20	2.2 ± 0.8	42.7 ± 4.6
1:10	7.3 ± 0.2	7.4 ± 0.3	10 ± 0.4	2.27 ± 0.02	45.2 ± 0.5
1:100	7.0 ± 0.4	9.9 ± 0.8	14 ± 1.5	2.48 ± 0.01	44.4 ± 0.5
1:1000	9.7 ± 0.1	3.2 ± 0.1	3.3 ± 0.1	2.12 ± 0.01	47.7 ± 0.5
1:2500	10.9 ± 0.2	3.3 ± 0.1	2.8 ± 0.1	2.01 ± 0.01	48.1 ± 0.5

[a]Errors are the parameter standard deviations from the fitting procedure.

scattering brightness on the known change of an analyte bulk refractive index; the difference in refractive index between single and double concentrated PBS was independently measured by a refractometer as 1.8×10^{-3} refractive index units (RIU). These data allowed us to convert relative brightness response into a scale equivalent to refractive index change; conventionally, this is given in response units, RU $\equiv 10^{-6}$ refractive index units.[38] The sensitivity of each array spot is typically 8×10^{-5} RIU, and the assays are averaged over 8 to 24 spots as required for multiplexed results. The responses from the spots functionalized with the same target molecules are averaged and referred to as "channels". The nonglycosylated BSA channel served as a nonspecific control. The analyte concentrations used in the assay were 27 mg/L for ConA and WGA; the rest of lectins were used at a concentration of 18 mg/L. The volume flow rate during the kinetic measurements was 50 μL/min.

A typical binding experiment procedure is shown in Figure 2A: (i) the baseline plasmon scattering intensity is recorded in the flow of running PBST buffer; (ii) the lectin sample solution was injected over the surface for approximately 200 s to record the association binding phase with sufficient accuracy to determine the association rate constant, k_a; (iii) the flow was switched to running buffer, and the dissociation phase kinetics were recorded for approximately 10 min; and (iv) the sensor was regenerated with 100 mM phosphoric acid solution.

The regeneration step (iv) removes the adsorbed analyte material from the assay spot and allows the array to be reused two or three times without loss of sensitivity or specificity. This allows assays to be repeated several times on the same sensor array without noticeable degradation in performance. No significant degradation of the sensor surface activity was observed after ten regeneration cycles. The assay is repeated with several concentrations of the target binding lectin and the kinetic data subjected to a global fit for both the association and dissociation phases simultaneously for all concentrations; from this, the binding rate constants can then be determined. An example of the experimental data is shown in Figure 2B where ConA binds specifically to αMan and the PFG functionalized sensor surfaces. The rest of the monosaccharide channels, βGal, βGlc, and βGlcNAc, do not show any affinity toward the ConA analyte, as expected, since ConA is only selective toward sugars in α-form.[39−41] Qualitative comparison of the responses in αMan and PFG channels revealed that although the rate of association with fibrinogen is slower the dissociation is also markedly slower than in the αMan channel.

RESULTS

Lectin-Monosaccharide Assays. A preliminary series of experiments was performed to establish sensitivity and selectivity of the lectin-saccharide assays using sensor arrays functionalized according to the legend shown in Figure 1B. The αMan and βGlcNAc saccharides are known to bind selectively to ConA and WGA, respectively.[40,42] The specific binding interactions between the modified sugars printed onto the array with the lectins ConA and WGA were studied over a range of lectin concentrations. The concentration-dependence series of kinetic binding responses were globally fitted (simultaneously for all analyte concentrations with a single set of kinetic parameters) with a 1:1 interaction model, described by the following equations:

dx.doi.org/10.1021/ac402872t | Anal. Chem. 2014, 86, 621−628

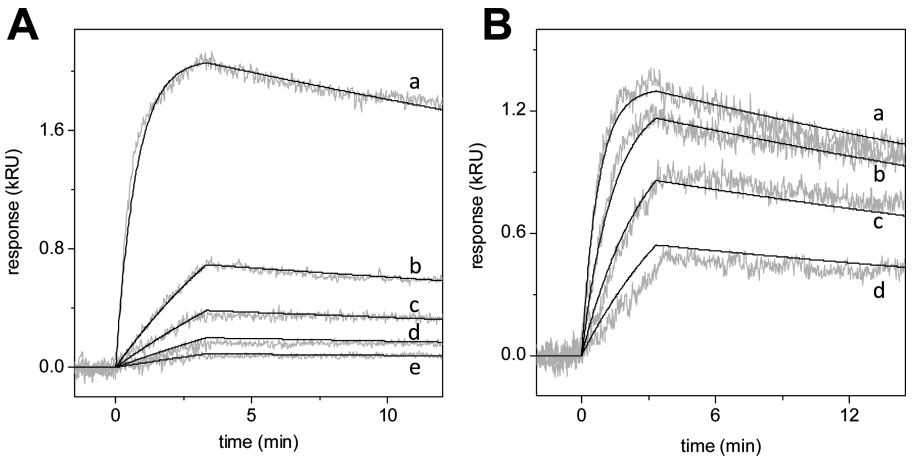

Figure 3. Global fit for the specific binding of the lectins to the sugars tethered on the surface with SAM linker/spacer ratio of 1:1000, assuming a 1:1 interaction model: (A) ConA-αMan binding with ConA concentrations (a) 24, (b) 2.3, (c) 1.2, (d) 0.57, and (e) 0.25 μg/mL; (B) WGA-βGlcNAc with WGA concentrations (a) 1.2, (b) 0.62, (c) 0.30, and (d) 0.15 μg/mL.

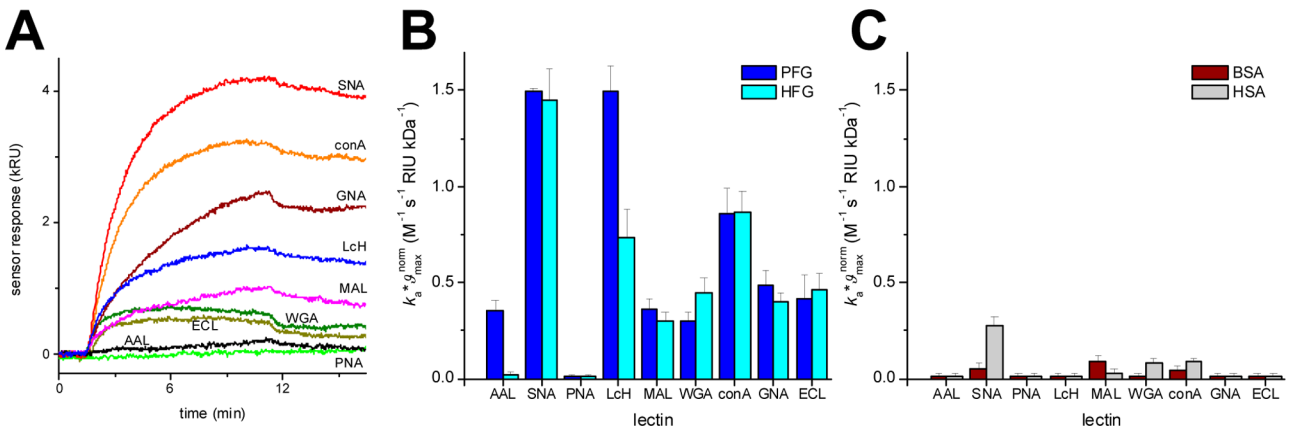

Figure 4. Lectin-HFG binding assays. (A) Kinetic traces of SNA, ConA, GNA, LcH, MAL, WGA, AAL, ECL, and PNA lectins binding to HFG sensors channel. One lectin was injected at a time, and the surface was regenerated after each incubation step. BSA sensor channel was used as nonglycosylated reference. (B) Comparison of the binding patterns observed in lectin assays of human and porcine fibrinogens: although the core structure of both glycans is similar, the prominent difference in AAL and LcH channels indicates that porcine glycan is fucosylated while the human one is not. (C) Binding patterns observed in the lectin assays of human and bovine serum albumins.

$$\text{association: } \vartheta(t) = \vartheta_m \frac{k_a[A]}{k_a[A] + k_d}(1 - e^{-(k_a[A]+k_d)t})$$

$$\text{dissociation: } \vartheta(t) = \vartheta_a e^{-k_d t}$$

where $[A]$ is the concentration of an analyte, k_a is the association rate constant, k_d is the dissociation rate constant, ϑ_m is the response to maximum analyte surface coverage, and ϑ_a is the analyte coverage achieved in association phase. The obtained parameters for the ConA-αMan binding on a set of sensor surfaces with varying linker/spacer SAMs are listed in Table 1. The thermodynamic equilibrium dissociation constants K_D may then be derived from the fitted rate constants: $K_D = k_d/k_a$.

The specific responses observed for lectin-monosaccharide pairs of ConA-αMan and WGA-βGlcNAc are shown in Figure 3 with their corresponding simulations from the global fit analyses. For the lower concentrations of both lectins, the 1:1 binding model shows a good fit to the data. At higher ConA concentrations, Figure 3A(a), the quality of the 1:1 model fit begins to deteriorate but χ^2 can be improved by 40% by allowing a second binding process to be incorporated as a double-exponential fit to the data.

The sensitivity of the assays may be assessed for the 200 s injection time indicating a detection limit of 10 ng/mL or 0.23 nM for WGA and 100 ng/mL or 0.93 nM for ConA. These values compare favorably with other techniques; for example, the bulk phase mannose glyco-conjugated nanoparticle-based absorption and scattering measurements were shown to have ConA limits of detection of 2−3 nM.[43]

The deviations from the 1:1 model indicated a more complex avidity interaction at high surface concentrations of lectin and sugars, so we have performed a series of experiments to determine the variation of the kinetic and thermodynamic parameters for the interactions between the lectins and different densities of sugars on the surface. The sugar surface density and therefore the potential for multiple lectin-sugar interactions was varied by varying the SAM composition achieved by changing the linker/spacer ratio. The variation of the association and dissociation rate constants for the ConA-αMan interactions is summarized in Table 1: the binding efficiency drops considerably when linker/spacer ratio is more than 1:1000. Also, the sensor surfaces with 1:1000 linker/spacer

dx.doi.org/10.1021/ac402872t | Anal. Chem. 2014, 86, 621−628

Table 2. Lectin-Fibrinogen Binding Parameters[a]

	PFG			HFG		
lectin	$10^{-3} \times k_a$ (M^{-1} s^{-1})	$10^4 \times k_d$ (s^{-1})	$k_a\vartheta_{max}^{norm}$ rate (M^{-1} s^{-1} RIU kDa^{-1})	$10^{-3} \times k_a$ (M^{-1} s^{-1})	$10^4 \times k_d$ (s^{-1})	$k_a\vartheta_{max}^{norm}$ rate (M^{-1} s^{-1} RIU kDa^{-1})
AAL	24.1 ± 4.3	5.1 ± 0.3	0.35 ± 0.06			
SNA	59.9 ± 5.4	2.0 ± 0.1	1.49 ± 0.02	58.0 ± 9.1	2.1 ± 0.1	1.45 ± 0.16
PNA						
LcH	24.2 ± 0.8	2.3 ± 0.1	1.49 ± 0.14	21.2 ± 4.4	8.9 ± 0.2	0.74 ± 0.15
MAL	8.78 ± 3.4	1.6 ± 0.2	0.36 ± 0.06	14.3 ± 5.6	12 ± 1	0.30 ± 0.05
WGA	16.5 ± 5.4	8.7 ± 0.2	0.30 ± 0.05	25.4 ± 6.2	24 ± 2	0.44 ± 0.08
ConA	28.0 ± 6.5	1.9 ± 0.1	0.86 ± 0.13	29.4 ± 8.0	2.5 ± 0.1	0.87 ± 0.10
GNA	8.71 ± 4.5	2.7 ± 0.1	0.49 ± 0.08	7.72 ± 4.7	4.6 ± 0.2	0.40 ± 0.05
ECL	38.2 ± 9.9	15 ± 5	0.42 ± 0.13	43.2 ± 12.3	26 ± 2	0.47 ± 0.08

[a]Errors correspond to the parameter variation from two repeats of the experiment.

SAMs showed the best responses in terms of signal-to-noise ratio and a good maximum lectin surface coverage.

The WGA-βGlcNAc binding on the sensor with a 1:1000 linker/spacer SAM is noticeably faster and stronger than ConA-αMan and characterized by the following kinetic and thermodynamic parameters: $k_a = (7.8 \pm 0.1) \times 10^5$ s^{-1} M^{-1}, $k_d = (3.2 \pm 0.1) \times 10^{-4}$ s^{-1}, $K_D = 0.41 \pm 0.05$ nM, and $\Delta G = 52.7 \pm 0.5$ kJ M^{-1}. After the sensitivity and selectivity of the sensor arrays were established, a series of assays was performed to illustrate the potential application of the technique in glycosylation characterization of proteins. Two fibrinogens, human and porcine, and two serum albumins, human and bovine, were coupled to the sensor surface on the SAMs with a 1:1000 linker/spacer dilution and subsequently interrogated with nine different lectins.

Lectin-Fibrinogen Assays. A nine-lectin screen was performed on the porcine and human fibrinogen glycoproteins using sensor arrays functionalized according to the legend shown in Figure 1C. An example of the obtained kinetic data for the interaction of lectins with HFG is shown in Figure 4A. Much more significant binding was observed on the fibrinogen compared to the BSA channels during the experiments since fibrinogen is a well-known glycosylated protein,[44] while albumin is not enzymatically glycosylated. The strongest specific binding to both HFG and PFG was observed for SNA and ConA lectins; in addition, specific binding was observed for LcH, MAL, WGA, GNA, and ECL, Figure 4A.

The lectin-fibrinogen binding sensogram data were analyzed, and the derived parameters are listed in Table 2. For visual comparison, the lectin binding rates can conveniently be presented in the form of a product of the association rate constant and the surface coverage, normalized with the lectin molecular mass: $k_a\vartheta_{max}^{norm}$.

The spectrum of the specific binding rates for the nine lectins used with a particular protein then form a characteristic pattern: Figure 4 shows the observed binding patterns for two fibrinogens (panel B) and two albumins (panel C). The most prominent difference between the binding in human and porcine fibrinogen channels was in binding LcH and AAL lectins, Figure 4B, suggesting that only the porcine glycan has fucosylated core regions. The BSA pattern shows three weak responses above the experimental noise level (from SNA, MAL, and ConA), all significantly smaller than the fibrinogen responses, thus justifying the use of BSA as a nonglycosylated reference.

Discussion. The aim of the current work was to assess the potential of an array-based, label-free particle plasmon screening technology for the rapid assessment of the posttranslational modification of proteins, specifically glycosylation. The aminoethyl glycosides were coupled to the carboxyl groups in SAMs allowing the surface sugar concentration to be varied by changing the linker/spacer ratio. Lower sugar surface densities are expected to result in a smaller number of binding sites on the surface reflecting simple 1:1 lectin-sugar binding kinetics. The kinetic parameters in Table 1 indicate a trend for a consistent determination and reproducibility especially in the dissociation rate constant, k_d, and hence the determination in K_D and the energy of interaction, with an apparent threshold at a 1:1000 linker/spacer ratio. The number of lectins bound to the surface derived from the fitted surface coverage, ϑ_m, however, showed variations of only 20%. The theoretical separation between linker/spacer molecules in the SAM is 0.45 nm[45,46] with the linker-linker separations in a rectangular matrix changing with increasing dilution: 0.9, 1.4, 4.5, 14.2, and 22.5 nm for 1:4, 1:10, 1:100, 1:1000, 1:2500 respectively. The distance between saccharide binding pockets of ConA is about 7.0 ± 0.5 nm,[47] which is 2−3-fold less than ideal interlinker distance. Although this may suggest that ConA would bind only one site for the linker/spacer ratios 1:1000 and 1:2500, the realistic SAM with randomly distributed linker molecules offers an ample amount of closer spaced sugars. Therefore two-site binding is reasonable, suggesting that the reported K_Ds are two-sites interaction avidity constants rather than affinity. Moreover, there is the fluidity within the SAM, and a lectin may recruit additional binding sugars once bound to the initial site on the surface. The overall best performance of the sensor arrays with the 1:1000 linker/spacer SAM lead to their use in the following protein glycosylation assays.

It has been observed previously that the measured interactions between lectins and sugars depends on whether the sugar or the lectin is immobilized on the sensor surface and on whether the sugars are monomers or oligomers.[48−52] The derived ConA-αMan interaction parameters listed in Table 1 indicate that K_D is in a low nanomolar range, consistent with the expected values for the sugar surface.[48] In addition, aggregation of the lectins has been observed at higher concentrations with multilectin binding to the tethered-sugar surfaces,[48] this explains the onset of deviation of the 1:1 kinetic model from the observed responses at high lectin concentrations. The relevant equilibrium dissociation constants K_D for the tethered-lectin-(mannose containing saccharide) binding reported in thermodynamic studies are in the range of 50−770 μM for mono- and disaccharides,[39,53,54] and up to 750 nM for more complex longer and branched oligosaccharides.[39] This further indicates that the derived K_D for ConA-αMan and WGA-βGlcNAc interactions are avidity constants.

dx.doi.org/10.1021/ac402872t | Anal. Chem. 2014, 86, 621−628

All interactions, whether for the tethered monosaccharide or the sugar presented by the printed fibrinogen protein, showed K_D values of ~1−50 nM, Tables 1 and 3. The nature of the interactions between the lectins and the presentation of the sugars both on the surface and on the fibrinogen glycoprotein are not the same and are indicative of the glycosylation pattern in some way.[44] The lectins ConA and WGA interact with the terminal αMan and βGlcNAc monosaccharides, respectively, but specific binding also commonly occurs to two/three sugar long oligosaccharides. The lectin SNA showed specific binding to sialic acid moieties on surface proteins, including fibrinogen,[55,56] and LcH is known to bind to the fucosylated biantennary core region.[44] Although the terminal monosaccharides can always occur to a small degree due to the microheterogeneity in the protein glycosylation,[57] a more realistic assumption is that lectins interact with a part of the glycan structure that is bigger than a single sugar base. Individual lectin binding rate constants to both PFG and HFG agree within the error ranges, implying that they bind to analogous areas of the glycan sugar sequences.

Taking into account known binding specificity of the used lectins toward oligosaccharide structures, Table 3, and known structures of the human[34,36] and porcine[35] fibrinogen carbohydrate compositions, the observed binding pattern can be readily interpreted. Each used lectin can be mapped to the corresponding region of the glycan structure: the schematic diagram in Figure 5 illustrates this correspondence using the Oxford notation to represent the *N*-linked glycan composition and structure.[58]

Table 3. Lectin Molecular Weights and Oligosaccharide Binding Specificities[35,40]

lectin	molecular weight (kDa)	preferred sugar specificity
AAL	67	Fuc(α16)GlcNAc
SNA	140	NeuAc(α26)Gal
PNA	112	Gal(β13)GalNAc
LcH	50	aMan, Fuc(α16)GlcNAc-Asn
MAL	75	NeuAc(α23)Gal
WGA	43	Man(β14)GlcNAc(β14)GlcNAc
ConA	106	αMan, αGlu, branched Man
GNA	50	Man(α13)Man
ECL	54	terminal Gal(β14)GlcNAc

The single fucose in the PFG composition is the only prominent difference between porcine and human fibrinogen N-glycans, with fucosylated content in HFG about 16 times smaller than in PFG.[36] The presence of this extra fucose sugar base in PFG is apparent in AAL and LcH channels of the lectin binding patterns, Figure 4B. Both PFG and HFG were reported to have a small degree of *O*-glycosylation;[35,55,59] an example of such proposed *O*-glycan structure NeuAc(α23)Gal(β13)-GalNAc on PFG α-chain[35] is shown in Figure 5. Although the PNA lectin, specific to the Gal(β13)GalNAc moiety of this *O*-glycan structure, was used in the current study, it did not show any binding to fibrinogen channels, and therefore, it is not possible to confirm the presence of fibrinogen *O*-glycans in the used protein samples.

Most of the used lectins could only bind to a single glycan area except SNA/MAL that may interact with both terminal sialylated antennae of biantennary structure and LcH that has two binding sites on porcine N-glycan. The patterns in Figure 4 agree semiquantitatively with the expected stoichiometries of the N-glycan structures. In practice, the relative sensor responses to different lectins are not expected to be directly stoichiometric due to a number of reasons. The most prominent is the effect of the lectin molecular weight since the employed detection technique is mass sensitive: reported lectin molecular weights vary significantly in the literature. Less obvious is the impact of the binding kinetic parameters, which control the transient curve shape and the maximum achievable signal: even for two lectins of the same molecular weight, the different steric hindrance or binding site accessibility and variation in equilibrium dissociation constants result in different reachable analyte surface coverages and, hence, the sensor responses. A sophisticated quantitative analysis requires knowledge of kinetic parameters for all individual lectin-oligosaccharide interactions, which is currently not available but is a compelling target for future investigation.

CONCLUSIONS

A biophotonic scattering array screening technique was successfully employed to study lectin-glycan interactions. A lectin screen of the tethered porcine and human proteins shows characteristic patterns of lectin binding with K_D values significantly different from the single sugar binding. The patterns can readily be associated with the known structures of porcine and human N-glycans and reflect the differences in glycosylation between species. The current configuration of printed protein and lectin screening offer many advantages, notably, the use of small quantities of often precious glycoproteins which may be stored and reused when required. The arrays have potential to be a new, rapid, and inexpensive high-throughput screening technology to determine the pattern

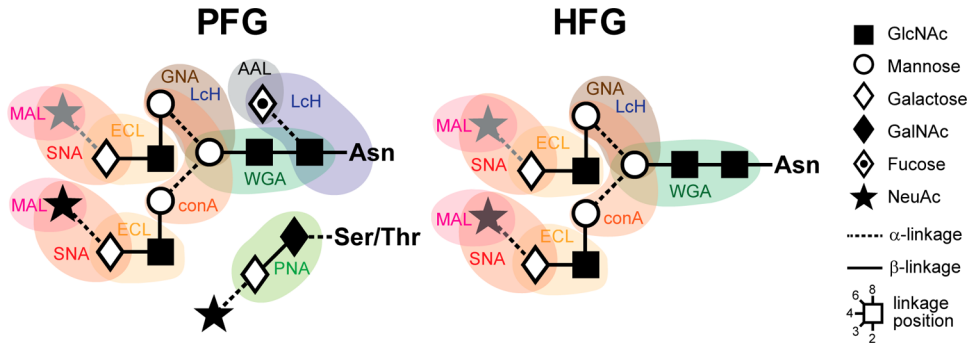

Figure 5. Structures of the porcine[35] and human[36] fibrinogen glycans in Oxford notation,[58] shaded areas indicate lectin-specific saccharide sequences, Table 3.

dx.doi.org/10.1021/ac402872t | Anal. Chem. 2014, 86, 621−628

of lectin binding which in turn can be used for structural glycosylation analysis and could therefore become a valuable tool in glycoscience, pharmaceutical research, and industry.

AUTHOR INFORMATION

Corresponding Author

*E-mail: andrew.m.shaw@exeter.ac.uk.

Notes

The authors declare no competing financial interest.

ACKNOWLEDGMENTS

The authors would like to thank Dr. Robert Sardzik for providing the aminoethyl galactose. This work was supported by the Royal Society (Wolfson Award to S.L.F.), the European Commission's Marie Curie program which funded the EuroGlycoArrays ITN (M.J.W.), and the EPSRC. R.V.O. would like to thank the BBSRC for support during this work.

REFERENCES

(1) Hourihane, J. O. B. *Pediatr. Clin. North Am.* **2011**, *58* (2), 445–458.
(2) Jefferis, R. *Trends Pharmacol. Sci.* **2009**, *30* (7), 356–362.
(3) Kayser, V.; Chennamsetty, N.; Voynov, V.; Forrer, K.; Helk, B.; Trout, B. L. *Biotechnol. J.* **2011**, *6* (1), 38–44.
(4) *Transforming Glycoscience: A Roadmap for the Future*; The National Academies Press: Washington, DC, 2012.
(5) Narhi, L. O.; Arakawa, T.; Aoki, K. H.; Elmore, R.; Rohde, M. F.; Boone, T.; Strickland, T. W. *J. Biol. Chem.* **1991**, *266* (34), 23022–23026.
(6) Li, H. J.; d'Anjou, M. *Curr. Opin. Biotechnol.* **2009**, *20* (6), 678–684.
(7) Jefferis, R.; Lefranc, M. P. *Mabs* **2009**, *1* (4), 332–338.
(8) Shin, I.; Park, S.; Lee, M. R. *Chem.—Eur. J.* **2005**, *11* (10), 2894–2901.
(9) Hartmann, M.; Lindhorst, T. K. *Eur. J. Org. Chem.* **2011**, *20–21*, 3583–3609.
(10) Walsh, C. T.; Garneau-Tsodikova, S.; Gatto, G. J. *Angew. Chem., Int. Ed.* **2005**, *44* (45), 7342–7372.
(11) Yoshida-Moriguchi, T.; Yu, L. P.; Stalnaker, S. H.; Davis, S.; Kunz, S.; Madson, M.; Oldstone, M. B. A.; Schachter, H.; Wells, L.; Campbell, K. P. *Science* **2010**, *327* (5961), 88–92.
(12) Arnold, J. N.; Wormald, M. R.; Sim, R. B.; Rudd, P. M.; Dwek, R. A. *Annu. Rev. Immunol.* **2007**, *25*, 21–50.
(13) Wada, Y.; Azadi, P.; Costello, C. E.; Dell, A.; Dwek, R. A.; Geyer, H.; Geyer, R.; Kakehi, K.; Karlsson, N. G.; Kato, K.; Kawasaki, N.; Khoo, K. H.; Kim, S.; Kondo, A.; Lattova, E.; Mechref, Y.; Miyoshi, E.; Nakamura, K.; Narimatsu, H.; Novotny, M. V.; Packer, N. H.; Perreault, H.; Peter-Katalinic, J.; Pohlentz, G.; Reinhold, V. N.; Rudd, P. M.; Suzuki, A.; Taniguchi, N. *Glycobiology* **2007**, *17* (4), 411–422.
(14) Slynko, V.; Schubert, M.; Numao, S.; Kowarik, M.; Aebi, M.; Allain, F. H. T. *J. Am. Chem. Soc.* **2009**, *131* (3), 1274–1281.
(15) Morelle, W. *Curr. Anal. Chem.* **2009**, *5* (2), 144–165.
(16) Antonopoulos, A.; North, S. J.; Haslam, S. M.; Dell, A. *Biochem. Soc. Trans.* **2011**, *39*, 1334–1340.
(17) Tanaka, H.; Fukuda, N.; Shoyama, Y. *J. Agric. Food. Chem.* **2007**, *55* (10), 3783–3787.
(18) Oguri, S. *Glycoconjugate J.* **2005**, *22* (7–9), 453–461.
(19) Weissenborn, M. J.; Castangia, R.; Wehner, J. W.; Sardzik, R.; Lindhorst, T. K.; Flitsch, S. L. *Chem. Commun.* **2012**, *48* (37), 4444–4446.
(20) Lis, H.; Sharon, N. *Chem. Rev.* **1998**, *98* (2), 637–674.
(21) Šardzík, R.; Green, A. P.; Laurent, N.; Both, P.; Fontana, C.; Voglmeir, J.; Weissenborn, M. J.; Haddoub, R.; Grassi, P.; Haslam, S. M.; Widmalm, G.; Flitsch, S. L. *J. Am. Chem. Soc.* **2012**, *134* (10), 4521–4524.
(22) Blixt, O.; Head, S.; Mondala, T.; Scanlan, C.; Huflejt, M. E.; Alvarez, R.; Bryan, M. C.; Fazio, F.; Calarese, D.; Stevens, J.; Razi, N.; Stevens, D. J.; Skehel, J. J.; van Die, I.; Burton, D. R.; Wilson, I. A.; Cummings, R.; Bovin, N.; Wong, C. H.; Paulson, J. C. *Proc. Natl. Acad. Sci. U. S. A.* **2004**, *101* (49), 17033–17038.
(23) Hirabayashi, J.; Yamada, M.; Kuno, A.; Tateno, H. *Chem. Soc. Rev.* **2013**, *42* (10), 4443–4458.
(24) Kuno, A.; Uchiyama, N.; Koseki-Kuno, S.; Ebe, Y.; Takashima, S.; Yamada, M.; Hirabayashi, J. *Nat. Methods* **2005**, *2* (11), 851–856.
(25) Karamanska, R.; Clarke, J.; Blixt, O.; MacRae, J. I.; Zhang, J. Q. Q.; Crocker, P. R.; Laurent, N.; Wright, A.; Flitsch, S. L.; Russell, D. A.; Field, R. A. *Glycoconjugate J.* **2008**, *25* (1), 69–74.
(26) Voglmeir, J.; Sardzik, R.; Weissenborn, M. J.; Flitsch, S. L. *Omics* **2010**, *14* (4), 437–444.
(27) Olkhov, R. V.; Shaw, A. M. *Biosens. Bioelectron.* **2008**, *23*, 1298–1302.
(28) Jansen van Vuuren, B.; Read, T.; Olkhov, R. V.; Shaw, A. M. *Anal. Biochem.* **2010**, *405* (1), 114–120.
(29) Ostuni, E.; Chapman, R. G.; Holmlin, R. E.; Takayama, S.; Whitesides, G. M. *Langmuir* **2001**, *17* (18), 5605–5620.
(30) Laurent, N.; Haddoub, R.; Voglmeir, J.; Wong, S. C.; Gaskell, S. J.; Flitsch, S. L. *ChemBioChem* **2008**, *9* (16), 2592–2596.
(31) Sardzik, R.; Noble, G. T.; Weissenborn, M. J.; Martin, A.; Webb, S. J.; Flitsch, S. L. *Beilstein J. Org. Chem.* **2010**, *6*, 699–703.
(32) Kiessling, L. L.; Splain, R. A. *Annu. Rev. Biochem.* **2010**, *79*, 619–653.
(33) Gestwicki, J. E.; Cairo, C. W.; Strong, L. E.; Oetjen, K. A.; Kiessling, L. L. *J. Am. Chem. Soc.* **2002**, *124* (50), 14922–14933.
(34) Townsend, R. R.; Hilliker, E.; Li, Y. T.; Laine, R. A.; Bell, W. R.; Lee, Y. C. *J. Biol. Chem.* **1982**, *257* (16), 9704–9710.
(35) L'Hôte, C.; Berger, S.; Bourgerie, S.; Duval-Iflah, Y.; Julien, R.; Karamanos, Y. *Infect. Immun.* **1995**, *63* (5), 1927–1932.
(36) Adamczyk, B.; Struwe, W. B.; Ercan, A.; Nigrovic, P. A.; Rudd, P. M. *J. Proteome Res.* **2012**, *12* (1), 444–454.
(37) Olkhov, R. V.; Fowke, J. D.; Shaw, A. M. *Anal. Biochem.* **2009**, *385*, 234–241.
(38) Kamat, P. V. *J. Phys. Chem. Lett.* **2009**, *1* (2), 520–527.
(39) Mandal, D. K.; Kishore, N.; Brewer, C. F. *Biochemistry* **1994**, *33* (5), 1149–1156.
(40) *Lectin and Lectin Conjugate, Catalog Addendum*; EY Laboratories: San Mateo, CA, 2006; Website: www.eylabs.com.
(41) *Table of Lectin Properties*; Vector Laboratories: Burlingame, CA, 2012; Website: www.vectorlabs.com.
(42) Bains, G.; Lee, R. T.; Lee, Y. C.; Freire, E. *Biochemistry* **1992**, *31* (50), 12624–12628.
(43) Watanabe, S.; Yamamoto, S.; Yoshida, K.; Shinkawa, K.; Kumagawa, D.; Seguchi, H. *Supramol. Chem.* **2011**, *23* (3–4), 297–303.
(44) Kollman, J. M.; Pandi, L.; Sawaya, M. R.; Riley, M.; Doolittle, R. F. *Biochemistry* **2009**, *48* (18), 3877–3886.
(45) Bareman, J. P.; Klein, M. L. *J. Phys. Chem.* **1990**, *94* (13), 5202–5205.
(46) Love, J. C.; Estroff, L. A.; Kriebel, J. K.; Nuzzo, R. G.; Whitesides, G. M. *Chem. Rev.* **2005**, *105* (4), 1103–1169.
(47) Sanders, D. A. R.; Moothoo, D. N.; Raftery, J.; Howard, A. J.; Helliwell, J. R.; Naismith, J. H. *J. Mol. Biol.* **2001**, *310* (4), 875–884.
(48) Duverger, E.; Frison, N.; Roche, A.-C.; Monsigny, M. *Biochimie* **2003**, *85* (1), 167–179.
(49) Shinohara, Y.; Sota, H.; Kim, F.; Shimizu, M.; Gotoh, M.; Tosu, M.; Hasegawa, Y. *J. Biochem.* **1995**, *117* (5), 1076–1082.
(50) Khan, M. I.; Sastry, M. V.; Surolia, A. *J. Biol. Chem.* **1986**, *261* (7), 3013–3019.
(51) Shinohara, Y.; Kim, F.; Shimizu, M.; Goto, M.; Tosu, M.; Hasegawa, Y. *Eur. J. Biochem.* **1994**, *223* (1), 189–194.
(52) Dai, Z.; Kawde, A.-N.; Xiang, Y.; La Belle, J. T.; Gerlach, J.; Bhavanandan, V. P.; Joshi, L.; Wang, J. *J. Am. Chem. Soc.* **2006**, *128* (31), 10018–10019.
(53) Houseman, B. T.; Mrksich, M. *Chem. Biol.* **2002**, *9* (4), 443–454.
(54) Schwarz, F. P.; Puri, K. D.; Bhat, R. G.; Surolia, A. *J. Biol. Chem.* **1993**, *268* (11), 7668–7677.

(55) Pacchiarotta, T.; Hensbergen, P. J.; Wuhrer, M.; van Nieuwkoop, C.; Nevedomskaya, E.; Derks, R. J. E.; Schoenmaker, B.; Koeleman, C. A. M.; van Dissel, J.; Deelder, A. M.; Mayboroda, O. A. *J. Proteomics* **2012**, *75* (3), 1067−1073.
(56) Wu, P. G.; Lee, K. B.; Lee, Y. C.; Brand, L. *J. Biol. Chem.* **1996**, *271* (3), 1470−1474.
(57) Harmon, B. J.; Gu, X.; Wang, D. I. C. *Anal. Chem.* **1996**, *68* (9), 1465−1473.
(58) Harvey, D. J.; Merry, A. H.; Royle, L.; Campbell, M. P.; Dwek, R. A.; Rudd, P. M. *Proteomics* **2009**, *9* (15), 3796−3801.
(59) Zauner, G.; Hoffmann, M.; Rapp, E.; Koeleman, C. A. M.; Dragan, I.; Deelder, A. M.; Wuhrer, M.; Hensbergen, P. J. *J. Proteome Res.* **2012**, *11* (12), 5804−5814.